



Modified transfer matrix method for steady-state forced vibration: a system of beam elements*

Andres Lahe

Department of Civil Engineering and Architecture, Tallinn University of Technology, Ehitajate tee 5, 19086 Tallinn, Estonia;
andres.lahe@ttu.ee

Received 23 March 2020, accepted 8 June 2020, available online 10 July 2020

© 2020 Author. This is an Open Access article distributed under the terms and conditions of the Creative Commons Attribution-NonCommercial 4.0 International License (<http://creativecommons.org/licenses/by-nc/4.0/>).

Abstract. The EST (Elements by a System of Transfer equations) method offers exact solutions for various vibration problems of trusses, beams and frames. The method can be regarded as an improved or modified transfer matrix method where the roundoff errors generated by multiplying transfer arrays are avoided. It is assumed that in a steady state a beam will vibrate with the circular frequency of an excitation force. The universal equation of elastic displacement (4th order differential equation) is described as a system of first order differential equations in matrix form. For the differential equations, the compatibility conditions of a beam element displacements at joint serve as essential boundary conditions. As the natural boundary conditions at joints, the equilibrium equations of elastic forces of beam elements are considered. At the supports, restrictions to displacements (support conditions) have been applied. For steady-state forced vibration, the phenomena of dynamic vibration absorption near the saddle points are observed, and the response curves for displacement amplitude and elastic energy are calculated.

Key words: steady-state forced vibrations, frequency response curves, dynamic vibration absorption, forcing functions, transfer equations, essential dynamic boundary conditions at joints, natural boundary conditions at joints, dynamic support conditions.

1. INTRODUCTION

One of the problems in structural engineering has been predicting the response of a structure or mechanical system to external steady-state forced vibration [2]. Two phenomena, resonance and dynamic vibration absorption, have been of great interest [3,4].

In computational structural mechanics the state-space representation of mechanical systems can be seen as an application of the transfer matrix method [5–9]:

$$\mathbf{Z}_L = \mathbf{U} \cdot \mathbf{Z}_A + \mathbf{Z}_p, \quad (1)$$

where

\mathbf{Z}_A , \mathbf{Z}_L designate the components (displacements, internal forces) of the state vectors at the beginning ($x = 0$) and end ($x = \ell$) of the element;

\mathbf{Z}_p is the element loading vector;

\mathbf{U} denotes the transfer matrix.

* A sequel to “Modified transfer matrix method for steady-state forced vibration: a system of bar elements” [1].

The forces are classified into internal (elastic and dissipative) and external (conservative and non-conservative) [10, p. 50; 11, p. 529].

An external force can be added as an element load (described by a forcing function) or as a nodal load on joints. The *general solution* to an ordinary differential equation can be obtained by adding a *particular solution* gained by the forcing function [12] to the *solution of a homogeneous equation*.

The forcing function for the linear time periodic (LTP) system [13] is dealt with in [14, p. 121; 15; 16; 17, p. 248; 9, pp. 26, 93, 94]. For input, the harmonic transfer function [18; 19, pp. 2, 3] with fundamental or pumping frequency [20, p. 48] has been used.

If there is a constraint force (load on joint) on the node, we have a problem with non-homogeneous boundary conditions that can be converted to an equivalent problem with homogeneous boundary conditions [21, p. 57; 22, p. 43].

Let us regard a set of transfer equations (similar to Eq. (1)) interconnected through the boundary conditions to a complete system:

$$\mathbf{spA}(\omega) \cdot \Phi = -\dot{\mathbf{Z}}, \quad (2)$$

where the vector Φ components Φ_k ($k = 1, 2, \dots, N$) are unknown state vectors of element ends and support reactions, where state vectors Z_A and Z_L components are Φ_i ($i = 1, 2, \dots, n$) and dynamic support reactions are $C_j \equiv \Phi_{n+j}$ ($j = 1, 2, \dots, m$), $n + m = N$. The term $\mathbf{spA}(\omega)$ is an augmented transfer matrix. The right-hand side $\dot{\mathbf{Z}}$ (*global loading vector*) of the equation system contains *element loading* vectors \mathbf{Z}_p and *nodal loads*. Boundary conditions play an important role for transfer equations [23, p. 1115]. The beam elements in Eq. (2) are interconnected through boundary conditions¹ [8, pp. 34–48]:

- compatibility equations of the displacements at nodes (geometric/essential boundary condition);
- joint equilibrium equations at nodes (natural boundary condition);
- side conditions (for bending moment, axial and shear force hinges);
- support conditions (restrictions on support displacements).

Here, by the improved or modified transfer matrix method, unlike the transfer matrix method (TMM) [2; 25, p. 236], transfer matrices are not multiplied to find the initial parameters (state vectors) [8, p. 49]. Hence the roundoff errors generated by multiplying transfer arrays are avoided. We will *scale up* (multiply) the displacements by the scaling multiplier. After solving the system of linear equations, we *scale down* (unscale) the initial parameter vectors of the elements dividing each of the displacements found by the scaling multiplier.

In a modal analysis, for the system of equations (2) the load vector is set to zero [26, eq. (31)]:

$$\mathbf{spA}(\omega_i) \cdot \Phi_i = 0. \quad (3)$$

For the nontrivial solution Φ_i of the homogeneous system (3), we will choose a free variable in accordance with the natural frequency ω_i :

$$\det(\mathbf{spA}(\omega_i)) = 0. \quad (4)$$

Here ω_i denotes different natural (or characteristic, or normal) frequencies that are found numerically by the bisection method. These values are conventionally arranged in sequence from smallest to largest ($\omega_1 < \omega_2 < \dots < \omega_n$).

For all the frequencies picked out from Eq. (4), the given boundary conditions and transfer equations are met.

¹ Euler–Bernoulli beam elements interconnected through boundary conditions are also considered in system-level modeling of microelectromechanical systems [24, p. 157].

The mode shapes are calculated according to Eq. (3), where the column of free variables is shifted to the right-hand side, and the system of equations obtained is solved with the least-squares method. After finding the initial parameters, we compile the mode shapes.

Free vibrations of beams with *boundary* and *initial conditions* are dealt with in [27].

To sustain vibration, energy must be supplied or transferred out. Two phenomena, resonance and dynamic vibration absorption, are of importance in steady-state forced vibrations [28]. On the frequency axis of steady-state forced vibration response curves, singular points – star and saddle points – lie [28; 29, p. 143].

The total response is the sum of the homogeneous and forced responses [20, p. 62]. For resonant frequency identification, the fundamental input frequency ω_p (pumping frequency for particular solution) is used [13, p. 4; 19, pp. 2, 3; 30].

In the saddle points of a LTP system, dynamic vibration absorption occurs.

2. STEADY-STATE FORCED VIBRATION OF BEAMS

Consider the free body diagram of a differential element of the beam in Fig. 1, where $\ddot{w} = \partial^2 w / \partial t^2$.

We will apply d’Alembert’s principle to extract the partial differential equation for transverse vibration of an elastic beam:

$$\Sigma M_2 = 0; \quad dM - Q_z dx + \underbrace{(p_z(x,t) - m\ddot{w}) dx^2 / 2}_{\text{higher order values}} = 0, \tag{5}$$

$$\Sigma Q_z = 0; \quad dQ + (p_z(x,t) - m\ddot{w}) dx = 0, \tag{6}$$

where $m = \rho A$ with ρ as the mass density and A as the cross sectional area of the beam element.

Now the Euler–Bernoulli hypotheses are used. The constitutive law for the beam relating the displacements $w(x)$ (curvature $d^2 w / dx^2$) and the bending moment M_y is

$$\frac{d^2 w}{dx^2} = -\frac{d\phi_y}{dx} = -\frac{1}{EI_y} M_y, \tag{7}$$

where EI_y is the bending stiffness of the beam. Combining Eqs (5), (6) and (7), we get (cf. [31, p. 1029])

$$\frac{\partial^2}{\partial x^2} EI_y \frac{\partial^2 w}{\partial x^2} + m \frac{\partial^2 w}{\partial t^2} = p_z(x,t). \tag{8}$$

Let us suppose that for the solution $w(x,t)$, space and time given as separated functions (cf. [32, pp. 9–10; 33, eq. (8); 34, p. 21; 27]):

$$w(x,t) = f(x) e^{i\theta t}. \tag{9}$$

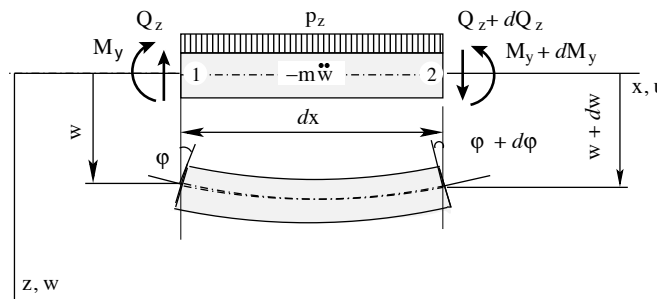


Fig. 1. Inertial force acting on a differential beam element.

Here $f(x)$ is a function of the independent variable x , and in the general case, θ is a complex frequency:

$$\theta = \omega + i\zeta_\omega, \quad (10)$$

where $\omega = \text{Re}(\theta)$ and $\zeta_\omega = \text{Im}(\theta)$ (see double imaginary characteristic roots on a complex plane [35, p. 29; 36; 37]). At steady-state vibration, $\text{Im}(\theta)$ describes: 1) in time-domain, the absence of damping, and 2) in frequency-domain, a phase-angle jump (PAJ) at natural frequencies (cf. [38]). The couplings between the frequencies of input and output signals can be taken into account [20,39,40; 41, pp. 13–14; 42].

Here the stability of a system is held together with its equilibrium state: a) at negative values of $\zeta_\omega < 0$, the slightly disturbed equilibrium state remains stable; b) at positive values of $\zeta_\omega > 0$, the slightly disturbed equilibrium state becomes unstable; c) at zero values of $\zeta_\omega = 0$ (see *sign principle* [43, p. 444; 44]), the equilibrium state remains neutral/indifferent, the system is *marginally stable*.

If the loading is given as $p_z(x, t) = q_z(x) e^{i\varpi t}$ [32, p. 21; 45, eq. (15); 33, eq. (6)], then substituting Eq. (9) into Eq. (8) gives

$$\left[EI_y \frac{d^4 f(x)}{dx^4} - \omega^2 \rho A f(x) \right] e^{i\theta t} = q_z(x) e^{i\varpi t}. \quad (11)$$

Here ϖ denotes the driving circular frequency.

After incorporating, at position x_a , the concentrated force $F_z(x) \delta(x - x_a) e^{i\varpi t}$ and the concentrated moment $\mathcal{M}_y(x) \delta^{(1)}(x - x_a) e^{i\varpi t}$ into Eq. (11), we obtain

$$\left[EI_y f^{IV}(x) - \rho A \omega^2 f(x) \right] = \left[q_z(x) + F_z(x) \delta(x - x_a) + \mathcal{M}_y(x) \delta^{(1)}(x - x_a) \right] e^{i\varpi t - i\theta t}, \quad (12)$$

where

$F_z(x) \delta(x - x_a)$ is a distributed force equivalent to a concentrated force (cf. [46, eq. (6)]);

$\mathcal{M}_y(x) \delta^{(1)}(x - x_a)$ is a distributed force equivalent to a concentrated moment (cf. [46, eq. (7)]);

$\delta(x - x_a)$ is the Dirac delta function;

$\delta^{(1)}(x - x_a)$ is the first distributional derivative of the Dirac delta function [46, eq. (5)].

We start counting the coordinate at $x = x_o = 0$ and time at $t = t_o = 0$ when the steady state frequency is same as the driving frequency (cf. differential equation being described as a system of first order differential equations [34, p. 29]). The natural exponential function is equal to 1 if $\exp(i(\varpi - \theta)t) = 1$; it means that there are two possibilities: $t = t_o = 0$ (cf. initial conditions in [27, p. 11]), or at $0 < t \leq nT$, where T is a period of vibration, the condition

$$\widehat{G} = i[\varpi - \omega] + \zeta_\omega = 0 \quad (13)$$

must be satisfied (cf. boundary conditions [27, p. 11]).

Let us start our investigation with a neutral/indifferent equilibrium ($\zeta_\omega = 0$, see the *sign principle*). The zero values of $\zeta_\omega = \text{Im}(\omega) = 0$ divide the parameter space into regions by the stability.

In frequency-domain we take the circular frequency $\omega = \varpi$ ($\varpi \neq \omega_n$, where ω_n denotes the natural frequency). The *crossing boundaries* $\omega^- = \omega_n - \varepsilon$ and $\omega^+ = \omega^- + \Delta\omega_n$ ($\Delta\omega_n$ marks a *phase shift* or *phase-angle jump*) divide the space into regions [36, fig. 2; 47; 48].

If the area A and moment of inertia I_y of the beam cross-section are constant, then using the assumption of Eq. (13), we get from the differential equation (12) a non-homogeneous 4th order differential equation to find the amplitudes of *steady-state output response* [20, p. 62]:

$$f^{IV}(x) - \frac{\omega^2 \rho A}{EI_y} f(x) = \frac{q(x)}{EI_y} + \frac{F_z(x) \delta(x - x_a)}{EI_y} + \frac{\mathcal{M}_y(x) \delta^{(1)}(x - x_a)}{EI_y}. \quad (14)$$

Equation (14) matches [33, eqs (9), (12)].

At steady-state forced vibration, for systems of periodically intermittent time [47] with $(n + 1)T \geq t \geq nT$, the frequencies ω_n lying on the abscissa axis of the amplitude-frequency-plane are given as singular points with $n = 1, 2, 3, \dots, N$ and $N \rightarrow \infty$ [28,49]. The isolated singular points are *star points*, and the double singular points are *saddle points*.

The homogeneous differential equation below serves to find eigenvalues and eigenvectors:

$$f^{IV}(x) - \frac{\omega^2 \rho A}{EI_y} f(x) = 0 \quad (15)$$

or

$$f^{IV}(x) - \kappa^4 f(x) = 0. \quad (16)$$

Here we use an auxiliary variable κ

$$\kappa^4 = \frac{\omega^2 \rho A}{EI_y} = \frac{\omega^2}{c^2}, \quad (17)$$

where κ represents the repeated roots of a characteristic (or frequency, or secular) equation of the linear differential equation for a beam:

$$\kappa_{1,2} = \sqrt[4]{\frac{\omega^2 \rho A}{EI_y}}, \quad \kappa_{3,4} = i \sqrt[4]{\frac{\omega^2 \rho A}{EI_y}}. \quad (18)$$

We have double real and double imaginary characteristic roots ($\kappa_{1,2}$ and $\kappa_{3,4}$, respectively) for dynamical systems [36,37].

Dimensionless eigenvalues

$$\lambda_n = \kappa \ell = \ell \sqrt[4]{\frac{\omega_n^2 \rho A}{EI_y}}, \quad (19)$$

where ℓ is the beam length.

To solve non-homogeneous linear ordinary differential equations of 4th order, e.g., Eq. (14), variation of parameters², also known as variation of constants, is a general method applied. The initial parameters method [50, eq. (142), p. 43; 51, p. 5; 52, p. 248 (LMC³ 126)] is also used.

The *basic equation (2) of the EST method* used in this paper may be considered as an improved transfer matrix method to find the state vectors, e.g., \mathbf{Z}_A and \mathbf{Z}_L in Eq. (1). Due to the *normed fundamental set of solutions*, the output parameters do not change the zero value of initial parameters at $x = 0$. Unlike the traditional transfer matrix method [2; 25, p. 236], here the transfer matrices are not multiplied to find the initial parameters. The novelty of this approach lies in the initial parameter vectors found by compiling sparse linear systems of equations incorporating *transfer equations* and *boundary conditions* (Eq. (2)) that are solved directly. Thus, the roundoff errors generated by multiplying transfer arrays are avoided.

First, we determine the state vectors \mathbf{Z}_A and \mathbf{Z}_L in Eq. (2) with the *basic equations of the EST method* [8, p. 49] that fit the solution of the homogeneous linear ordinary differential equation (15) (see [8, p. 33]). Further we calculate the *state vector* $\mathbf{Z}_L(\mathbf{x})$ in Eq. (2) which is consistent with the non-homogeneous equation (14). The EST method makes use of the variation of parameters to solve problems of steady-state forced vibrations as well as statics of structural systems with interconnected elements.

In order to solve Eq. (37), we need to find the loading vector \mathbf{Z}_p . The frequency ω at singular points has a phase-angle jump $\Delta\omega_n$ associated with *in-phase/out-of-phase* behaviour [53, slide 36]. The dimensionless frequency phase-angle jump $\Delta\lambda_k$ at singular points is also used. For sinusoidal response, a phase shift to the opposite phase is equal to π (*out-of-phase*) and a shift to the same phase is equal to 2π (*in-phase*).

A singular point is often associated with a sudden change in the system. In case of undamped harmonic loading, at response frequency, the amplitudes $f(x)$ at singular points may reach infinity (quality factor

² [https://math.libretexts.org/Bookshelves/Differential_Equations/Book%3A_Elementary_Differential_Equations_with_Boundary_Values_Problems_\(Trench\)/09%3A_Linear_Higher_Order_Differential_Equations/9.04%3A_Variation_of_Parameters_for_Higher_Order_Equations](https://math.libretexts.org/Bookshelves/Differential_Equations/Book%3A_Elementary_Differential_Equations_with_Boundary_Values_Problems_(Trench)/09%3A_Linear_Higher_Order_Differential_Equations/9.04%3A_Variation_of_Parameters_for_Higher_Order_Equations)

³ LMC – left mouse click.

$Q = \infty$), and a phase-angle jump occurs [54, p. 534; 55]. At star points, amplitude changes are significantly larger than at saddle points, where amplitude changes should be determined with low threshold or can be labelled as ‘positive’ versus ‘negative’ (see Fig. 10a) [55]. A saddle point phase portrait is shown in [56, p. 181 (LMC 199), fig. 4.7 (c)]. For steady-state forced vibration loading, dimensionless frequency phase-angle jumps $\Delta\lambda_k$ appear:

- at star points ($k = 1, 3, 5, \dots$);
- at saddle points ($k = 2, 4, 6, \dots$).

At singular points, the amplitude $f(x)$ sign changes into reverse (Fig. 10a) associated with the *in-phase/out-of-phase* behaviour [53, slide 36].

The general solution $f(x)$ of the non-homogeneous differential equation (14) can be expressed as a sum of the general solution $f_h(x)$ of the complementary equation (15) and the particular solution $f_e(x)$ of the non-homogeneous differential equation (14).

The fundamental set of solutions to the differential equation (16) has the form

$$f_1^*(\kappa x) = \text{ch}\kappa x, \quad f_2^*(\kappa x) = \text{sh}\kappa x, \quad f_3^*(\kappa x) = \cos \kappa x, \quad f_4^*(\kappa x) = \sin \kappa x. \tag{20}$$

We norm the fundamental set of solutions (20) so that the Wronskian $W(x)$ (normalized fundamental matrix) is the determinant of the identity matrix $I_{4 \times 4}$ at $x = 0$. The normed fundamental set of solutions for the homogeneous differential equation is given below [9, p. 67; 33, eq. (15)]:

$$f_1(\kappa x) = \frac{1}{2}(\text{ch}\kappa x + \cos \kappa x) = K_1(\kappa x), \tag{21}$$

$$f_2(\kappa x) = \frac{1}{2\kappa}(\text{sh}\kappa x + \sin \kappa x) = \frac{1}{\kappa}K_2(\kappa x), \tag{22}$$

$$f_3(\kappa x) = \frac{1}{2\kappa^2}(\text{ch}\kappa x - \cos \kappa x) = \frac{1}{\kappa^2}K_3(\kappa x), \tag{23}$$

$$f_4(\kappa x) = \frac{1}{2\kappa^3}(\text{sh}\kappa x - \sin \kappa x) = \frac{1}{\kappa^3}K_4(\kappa x). \tag{24}$$

The functions $K_i(\kappa x)$ are also called Krylov–Duncan functions [57, p. 192; 50, eq. (136), p. 42; 16, p. 543; 17, p. 247].

Krylov–Duncan functions and their derivatives satisfy permutations [57, p. 192; 17, p. 247] (see Tables 1 and 2).

Table 1. The cyclic order of Krylov–Duncan functions derivatives

Functions	Derivatives			
	First	Second	Third	Fourth
$K_1(\kappa x)$	$\kappa K_4(\kappa x)$	$\kappa^2 K_3(\kappa x)$	$\kappa^3 K_2(\kappa x)$	$\kappa^4 K_1(\kappa x)$
$K_2(\kappa x)$	$\kappa K_1(\kappa x)$	$\kappa^2 K_4(\kappa x)$	$\kappa^3 K_3(\kappa x)$	$\kappa^4 K_2(\kappa x)$
$K_3(\kappa x)$	$\kappa K_2(\kappa x)$	$\kappa^2 K_1(\kappa x)$	$\kappa^3 K_4(\kappa x)$	$\kappa^4 K_3(\kappa x)$
$K_4(\kappa x)$	$\kappa K_3(\kappa x)$	$\kappa^2 K_2(\kappa x)$	$\kappa^3 K_1(\kappa x)$	$\kappa^4 K_4(\kappa x)$

Table 2. Initial values: derivatives of normed fundamental solutions at $x = 0$

Solution set	f_1	f_2	f_3	f_4
Function	1	0	0	0
1st derivative	0	1	0	0
2nd derivative	0	0	1	0
3rd derivative	0	0	0	1

The particular solution of Eq. (14), with zero initial value (zero state response), is obtained using the convolution integral [58, p. 156; 59, p. 279; 9, p. 92]

$$f_e(x) = \int_{x_0}^x G_n(x, \xi) g_n(\xi) d\xi \quad (25)$$

or, to be more precise,

$$f_e(x) = \int_{x_0}^x G_4(x, \xi) g_4(\xi) d\xi + \int_{x_0}^x G_3(x, \xi) g_3(\xi) d\xi + \int_{x_0}^x G_2(x, \xi) g_2(\xi) d\xi. \quad (26)$$

Here $G_n(x, \xi)$ is the normed fundamental set of solutions to the associated homogeneous differential equation, given by Eqs (21)–(24):

$$G_4(x, \xi) = f_4(x - \xi) = \frac{1}{2\kappa^3} (\text{sh}\kappa(x - \xi) - \sin \kappa(x - \xi)) = \frac{1}{\kappa^3} K_4(\kappa(x - \xi)), \quad (27)$$

$$G_3(x, \xi) = f_3(x - \xi) = \frac{1}{2\kappa^2} (\text{ch}\kappa(x - \xi) - \cos \kappa(x - \xi)) = \frac{1}{\kappa^2} K_3(\kappa(x - \xi)), \quad (28)$$

$$G_2(x, \xi) = f_2(x - \xi) = \frac{1}{2\kappa} (\text{sh}\kappa(x - \xi) + \sin \kappa(x - \xi)) = \frac{1}{\kappa} K_2(\kappa(x - \xi)). \quad (29)$$

The load function $g_n(\xi)$ from Eq. (25) is described with

$$g_4(\xi) = \frac{q_z(\xi)}{EI_y}, \quad g_3(\xi) = \frac{F_z(\xi)}{EI_y}, \quad f_2(\xi) = \frac{\mathcal{M}_y(\xi)}{EI_y} \quad (30)$$

(cf. Eq. (14)).

We get the following particular solutions, where the relationship $\lambda = \kappa\ell$ is taken into account and $x_a = a$.
For q_z

$$\begin{aligned} f_{4e}(x) &= \frac{q_z}{EI_y} \frac{1}{2\kappa^4} [\text{ch}\kappa\langle x-a \rangle_+ + \cos \kappa\langle x-a \rangle_+ - 2] \\ &= \frac{q_z}{EI_y} \frac{1}{\kappa^4} [K_1(\kappa\langle x-a \rangle_+) - 1] = \frac{q_z}{EI_y} \frac{\ell^4}{\lambda^4} [K_1(\kappa\langle x-a \rangle_+) - 1]. \end{aligned} \quad (31)$$

This particular solution compares well with solutions in [57, p. 197] and [2, p. 143].

For F_z

$$\begin{aligned} f_{3e}(x) &= \frac{F_z}{EI_y} \frac{1}{2\kappa^3} [\text{sh}\kappa\langle x-a \rangle_+ - \sin \kappa\langle x-a \rangle_+] \\ &= \frac{F_z}{EI_y} \frac{1}{\kappa^3} [K_4(\kappa\langle x-a \rangle_+)] = \frac{F_z}{EI_y} \frac{\ell^3}{\lambda^3} [K_4(\kappa\langle x-a \rangle_+)]. \end{aligned} \quad (32)$$

The present particular solution compares well with the solution in [14, p. 120].

For \mathcal{M}_y

$$\begin{aligned} f_{2e}(x) &= \frac{\mathcal{M}_y}{EI_y} \frac{1}{2\kappa^2} [\text{ch}\kappa\langle x-a \rangle_+ - \cos \kappa\langle x-a \rangle_+] \\ &= \frac{\mathcal{M}_y}{EI_y} \frac{1}{\kappa^2} [K_3(\kappa\langle x-a \rangle_+)] = \frac{\mathcal{M}_y}{EI_y} \frac{\ell^2}{\lambda^2} [K_3(\kappa\langle x-a \rangle_+)]. \end{aligned} \quad (33)$$

The particular solutions $f_{4e}(x)$, $f_{3e}(x)$, $f_{2e}(x)$ compare well with the equations in [33, eq. (23)] ($r_i = 0$).

According to I. M. Babakov [15], cited in [17, p. 248], the particular solutions including a harmonic force or moment are also called *Krylov's partial integrals*.

To create the loading vector $\mathbf{Z}_p = \mathbf{Z}_q + \mathbf{Z}_F + \mathbf{Z}_M$ of the transfer equations, we use the particular solutions (31), (32) and (33).

Loading vector components of a distributed force q_z :

$$\mathbf{Z}_q = \begin{bmatrix} \circledast w_e \\ \circledast \varphi_e \\ \circledast Q_e \\ \circledast M_e \end{bmatrix} = \begin{bmatrix} f_{4e} \\ -f'_{4e} \\ -EI_y f'''_{4e} \\ -EI_y f''_{4e} \end{bmatrix} = \begin{bmatrix} \frac{q_z}{EI_y} \frac{1}{\kappa^4} [K_1 (\kappa \langle x-a \rangle_+) - 1] \\ -\frac{q_z}{EI_y} \frac{1}{\kappa^3} [K_4 (\kappa \langle x-a \rangle_+)] \\ -\frac{q_z}{\kappa} [K_2 (\kappa \langle x-a \rangle_+)] \\ -\frac{q_z}{\kappa^2} [K_3 (\kappa \langle x-a \rangle_+)] \end{bmatrix}. \quad (34)$$

Loading vector components of a concentrated force F_z (cf. [14, eqs (6.65)–(6.68), p. 120]) [33, eq. (21)]:

$$\mathbf{Z}_F = \begin{bmatrix} \circledast w_e \\ \circledast \varphi_e \\ \circledast Q_e \\ \circledast M_e \end{bmatrix} = \begin{bmatrix} f_{3e} \\ -f'_{3e} \\ -EI_y f'''_{3e} \\ -EI_y f''_{3e} \end{bmatrix} = \begin{bmatrix} \frac{F_z}{EI_y} \frac{1}{\kappa^3} [K_4 (\kappa \langle x-a \rangle_+)] \\ -\frac{F_z}{EI_y} \frac{1}{\kappa^2} [K_3 (\kappa \langle x-a \rangle_+)] \\ -F_z [K_1 (\kappa \langle x-a \rangle_+)] \\ -\frac{F_z}{\kappa} [K_2 (\kappa \langle x-a \rangle_+)] \end{bmatrix}. \quad (35)$$

Loading vector components of a concentrated moment \mathcal{M}_y [33, eq. (21)]:

$$\mathbf{Z}_M = \begin{bmatrix} \circledast w_e \\ \circledast \varphi_e \\ \circledast Q_e \\ \circledast M_e \end{bmatrix} = \begin{bmatrix} f_{2e} \\ -f'_{2e} \\ -EI_y f'''_{2e} \\ -EI_y f''_{2e} \end{bmatrix} = \begin{bmatrix} \frac{\mathcal{M}_y}{EI_y} \frac{1}{\kappa^2} [K_3 (\kappa \langle x-a \rangle_+)] \\ -\frac{\mathcal{M}_y}{EI_y} \frac{1}{\kappa} [K_2 (\kappa \langle x-a \rangle_+)] \\ -\mathcal{M}_y \kappa [K_4 (\kappa \langle x-a \rangle_+)] \\ -\mathcal{M}_y [K_1 (\kappa \langle x-a \rangle_+)] \end{bmatrix}. \quad (36)$$

To describe the beam element shown in Fig. 2, we apply the right-handed coordinate system and sign convention 2.

Let us present the transfer equations for vibration of a Euler–Bernoulli beam (sign convention 2 is used):

$$\mathbf{Z}_L(\mathbf{x}) = \mathbf{U} \cdot \mathbf{Z}_A + \mathbf{Z}_p. \quad (37)$$

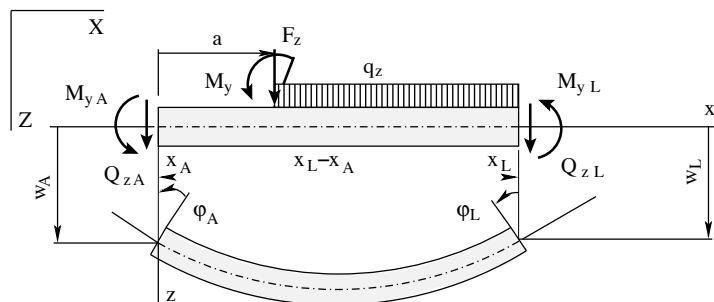


Fig. 2. Beam element with positive direction of displacements, rotations, forces and bending moments.



Fig. 3. Indices of state vector components for a beam element.

Components of the state vector are displacements, rotations, shear forces and bending moments at the ends of the element shown in Fig. 3.

$$\mathbf{Z}_A = \begin{bmatrix} w_A \\ \varphi_A \\ Q_A \\ M_A \end{bmatrix} = \begin{bmatrix} Z(1) \\ Z(2) \\ Z(3) \\ Z(4) \end{bmatrix}, \quad \mathbf{Z}_L = \begin{bmatrix} w_L \\ \varphi_L \\ Q_L \\ M_L \end{bmatrix} = \begin{bmatrix} Z(5) \\ Z(6) \\ Z(7) \\ Z(8) \end{bmatrix}. \tag{38}$$

The components of the state vector $Z(i)$ ($i = 1, 2, 3, \dots, 8$) (cf. $\Phi(i)$ in Eq. (2)) in index notation are brought in Fig. 3.

Here, to find the initial parameter vectors \mathbf{Z}_A , we improve or modify the transfer matrix method. In the traditional transfer matrix method, to find the initial parameters (state vectors) the transfer matrices are multiplied. To avoid the roundoff errors generated by multiplying transfer arrays, we will compile sparse linear systems of equations containing *transfer equations* and *boundary conditions*. With these sparse equations, designated by us as *the basic equations of the EST method*, we find the initial parameter vector \mathbf{Z}_A . The sparse equations (2) can be expressed as the basic equations of the EST method for a beam:

$$[\mathbf{U} - \mathbf{I}_{4 \times 4}] \begin{bmatrix} \mathbf{Z}_A \\ \mathbf{Z}_L \end{bmatrix} = -\mathbf{Z}_p, \tag{39}$$

hence

$$\widehat{\mathbf{U}}_{4 \times 8} \cdot \widehat{\mathbf{Z}} = -\mathbf{Z}_p. \tag{40}$$

Here \mathbf{Z}_p is the loading vector,

$$\widehat{\mathbf{Z}} = \begin{bmatrix} \mathbf{Z}_A \\ \mathbf{Z}_L \end{bmatrix}, \tag{41}$$

and $\widehat{\mathbf{U}}_{4 \times 8}$ is the augmented transfer matrix ($U_{4 \times 4} \mid -I_{4 \times 4}$):

$$\widehat{\mathbf{U}}_{4 \times 8} = \begin{bmatrix} K_1(\kappa\ell) & -\frac{1}{\kappa}K_2(\kappa\ell) & \frac{i_o}{EI} \frac{1}{\kappa^3}K_4(\kappa\ell) & \frac{i_o}{EI} \frac{1}{\kappa^2}K_3(\kappa\ell) & & & & \\ -\kappa K_4(\kappa\ell) & K_1(\kappa\ell) & -\frac{i_o}{EI} \frac{1}{\kappa^2}K_3(\kappa\ell) & -\frac{i_o}{EI} \frac{1}{\kappa}K_2(\kappa\ell) & & & & \\ -\frac{1}{i_o} EI \kappa^3 K_2(\kappa\ell) & \frac{1}{i_o} EI \kappa^2 K_3(\kappa\ell) & -K_1(\kappa\ell) & -\kappa K_4(\kappa\ell) & & & & \\ -\frac{1}{i_o} EI \kappa^2 K_3(\kappa\ell) & \frac{1}{i_o} EI \kappa K_4(\kappa\ell) & -\frac{1}{\kappa}K_2(\kappa\ell) & -K_1(\kappa\ell) & & & & \\ & & & & -1 & 0 & 0 & 0 \\ & & & & 0 & -1 & 0 & 0 \\ & & & & 0 & 0 & -1 & 0 \\ & & & & 0 & 0 & 0 & -1 \end{bmatrix}, \tag{42}$$

where ℓ is the length of the beam element, and i_o is the scaling multiplier for displacements and rotations (e.g., $i_o = 1.0$, $i_o = EI_{basic}/\ell_{basic}$).

In system (2), the first four equations represent the basic equation (39) of the EST method, the rest being boundary conditions.

The boundary conditions of a cantilever beam:

$$\begin{aligned} w_A &\equiv \Phi(1) = 0, \\ \varphi_A &\equiv \Phi(2) = 0, \\ Q_L &\equiv \Phi(7) = 0, \\ M_L &\equiv \Phi(8) = 0. \end{aligned} \quad (43)$$

Equated to zero, the determinant of the coefficient matrix of equations (39) (cf. Eq. (4)) – the boundary conditions of which are expressed by Eq. (43) (see [9, p. 72]) – allows us to form the frequency (or characteristic, or secular) equation for a cantilever beam. After reducing the determinant and substituting $\kappa\ell = \lambda$, we obtain the frequency equation (cf. [14, p. 110; 60, p. 527])

$$1 + \operatorname{ch}(\lambda) \cos(\lambda) = 0, \quad (44)$$

$$\lambda_1 = 1.8751040; \lambda_2 = 4.6940911; \lambda_3 = 7.8547574; \lambda_4 = 10.9955407; \lambda_5 = 14.1371684; \lambda_6 = 17.2787595.$$

The boundary conditions of a fixed-fixed beam:

$$\begin{aligned} w_A &\equiv \Phi(1) = 0, \\ \varphi_A &\equiv \Phi(2) = 0, \\ w_L &\equiv \Phi(5) = 0, \\ \varphi_L &\equiv \Phi(6) = 0. \end{aligned} \quad (45)$$

Equated to zero, the determinant of the coefficient matrix of equation (39) (cf. Eq. (4)) – the boundary conditions of which are expressed by Eq. (45) (see [9, p. 73]) – makes it possible to write the frequency (or characteristic, or secular) equation for a fixed-fixed beam. We obtain the frequency equation after reducing the determinant and substituting $\kappa\ell = \lambda$ (cf. [14, p. 109; 60, p. 527]):

$$\operatorname{ch}(\lambda) \cos(\lambda) - 1 = 0, \quad (46)$$

$$\lambda_1 = 4.7300407; \lambda_2 = 7.8532046; \lambda_3 = 10.9956078; \lambda_4 = 14.1371655; \lambda_5 = 17.2787597; \lambda_6 = 20.4203522.$$

The boundary conditions of a simply supported beam (with a pin connection on one end and a roller support on the other):

$$\begin{aligned} w_A &\equiv \Phi(1) = 0, \\ M_A &\equiv \Phi(4) = 0, \\ w_L &\equiv \Phi(5) = 0, \\ M_L &\equiv \Phi(8) = 0. \end{aligned} \quad (47)$$

Equated to zero, the determinant of the coefficient matrix of equation (39) (cf. Eq. (4)) – the boundary conditions of which are expressed by Eq. (47) (see [9, p. 74]) – makes it possible to write the frequency (or characteristic, or secular) equation for a simply supported beam. We obtain the frequency equation after reducing the determinant and substituting $\kappa\ell = \lambda$ (cf. [14, p. 108; 60, p. 527]):

$$\operatorname{sh}\lambda \sin\lambda = 0 \quad (\text{if } \lambda \neq 0, \text{ then } \sin\lambda = 0), \quad (48)$$

$$\lambda_1 = 3.141593; \lambda_{n+1} = \lambda_n + \pi \quad (n = 1, 2, 3, \dots).$$

The boundary conditions of a propped cantilever beam (fixed on one end, the free end resting on a roller support):

$$\begin{aligned} w_A &\equiv \Phi(1) = 0, \\ M_A &\equiv \Phi(4) = 0, \\ w_L &\equiv \Phi(5) = 0, \\ \varphi_L &= \Phi(6) = 0. \end{aligned} \quad (49)$$

Equated to zero, the determinant of the coefficient matrix of equations (39) (cf. Eq. (4)) – the boundary conditions of which are expressed by Eq. (49) (see [9, p. 75]) – allows us to form the frequency (or characteristic, or secular) equation for a propped cantilever beam. After reducing the determinant and substituting $\kappa\ell = \lambda$, we obtain the frequency equation (cf. [14, p. 110; 60, p. 527])

$$\text{ch}\lambda \sin \lambda - \text{sh}\lambda \cos \lambda = 0, \tag{50}$$

$\lambda_1 = 3.9266023$; $\lambda_2 = 7.0685827$; $\lambda_3 = 10.2101761$; $\lambda_4 = 13.3517687$; $\lambda_5 = 16.4933614$; $\lambda_6 = 19.6349541$.

The natural eigenvalues for beams, with different boundary conditions, found above are equal to the frequencies gained with the *Adomian decomposition method* (ADM) [61, table 1, p. 11].

Example 2.1 (steady-state forced vibration of a fixed-fixed beam). Compose the steady-state frequency response curves of a fixed-fixed beam. Find the amplitudes of displacements, angles of rotation, bending moments and shear forces of the beam in Fig. 4 under the excitation force $F_b e^{i\omega t}$.

The fixed-fixed beam is of length $\ell = 0.229\text{m}$; the distance a from the left end of the beam to point b is 0.1145m ; the cross-sectional height is 0.79mm and width 1.27cm ; elastic or Young’s modulus $E = 205\text{GN/m}^2$; shear modulus $G = 76.53228\text{GN/m}^2$; mass density $\rho = 7.870 \times 10^3\text{kg/m}^3$; $A_{red} = A/1.2$ (A is the cross-sectional area). The forcing amplitude $F_b = 0.889644\text{N}$ with frequencies $\omega_b = 376.99\text{s}^{-1} \cong f_b = 60\text{Hz}$ and $\omega_b = 628.32\text{s}^{-1} \cong f_b = 100\text{Hz}$ (cf. [62]).

The relationship between the angular frequency ω and dimensionless frequency λ is given by the formula (cf. [9, p. 77])

$$\omega_n = \frac{\lambda_n^2}{\ell^2} \sqrt{\frac{EI}{A\rho}} = \lambda_n^2 \sqrt{\frac{EI}{m\ell^4}}. \tag{51}$$

The system of EST-method equations (40) (cf. Eq. (2)) is

$$\text{spA} \cdot \mathbf{Z} = \dot{\mathbf{Z}}, \tag{52}$$

where \mathbf{Z} is the vector of unknowns:

$$\mathbf{Z} = \begin{bmatrix} \mathbf{Z}_a \\ \mathbf{Z}_c \end{bmatrix}. \tag{53}$$

The state vector input \mathbf{Z}_a and output \mathbf{Z}_c components are displacements and forces at the ends of the beam ac in Fig. 5:

$$\mathbf{Z}_a = \begin{bmatrix} w_A^{(ac)} \\ \varphi_A^{(ac)} \\ Q_A^{(ac)} \\ M_A^{(ac)} \end{bmatrix} \equiv \begin{bmatrix} Z(1) \\ Z(2) \\ Z(3) \\ Z(4) \end{bmatrix}, \quad \mathbf{Z}_c = \begin{bmatrix} w_L^{(ac)} \\ \varphi_L^{(ac)} \\ Q_L^{(ac)} \\ M_L^{(ac)} \end{bmatrix} \equiv \begin{bmatrix} Z(5) \\ Z(6) \\ Z(7) \\ Z(8) \end{bmatrix}. \tag{54}$$

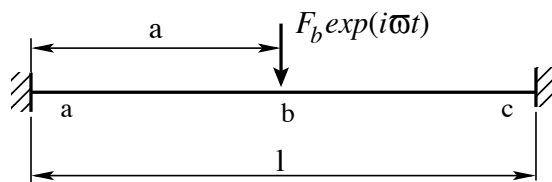


Fig. 4. Fixed-fixed beam.

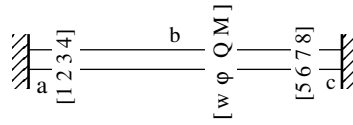


Fig. 5. Displacement and force indices of fixed-fixed beam element.

The components of the state vector $Z(i)$ ($i = 1, 2, 3, \dots, 8$) (cf. $\Phi(i)$ in Eq. (2)) in index notation are shown in Fig. 5.

In system (52), the first four equations represent the basic equation (39) of the EST method, the rest are boundary conditions:

$$\begin{aligned} w_A^{(ac)} &\equiv Z(1) = 0, \\ \varphi_A^{(ac)} &\equiv Z(2) = 0, \\ w_L^{(ac)} &\equiv Z(5) = 0, \\ \varphi_L^{(ac)} &\equiv Z(6) = 0. \end{aligned} \quad (55)$$

For nontrivial solutions of the homogeneous system (52), natural frequencies ω_i of the beam are found. Figure 6 illustrates the dependence of the determinant of the coefficient matrix of Eqs (52) on angular frequency ω of the beam.

The first eight natural frequencies of the fixed-fixed beam are: $\omega_1 = 496.574977 \text{ s}^{-1}$, $\omega_2 = 1368.828047 \text{ s}^{-1}$, $\omega_3 = 2683.450276 \text{ s}^{-1}$, $\omega_4 = 4435.879619 \text{ s}^{-1}$, $\omega_5 = 6626.438860 \text{ s}^{-1}$, $\omega_6 = 9255.108706 \text{ s}^{-1}$, $\omega_7 = 12321.888787 \text{ s}^{-1}$, $\omega_8 = 15826.801500 \text{ s}^{-1}$; $f_1 = 79.032 \text{ Hz}$, $f_2 = 217.86 \text{ Hz}$, $f_3 = 427.08 \text{ Hz}$, $f_4 = 705.99 \text{ Hz}$, $f_5 = 1054.6 \text{ Hz}$, $f_6 = 1473.0 \text{ Hz}$, $f_7 = 1961.1 \text{ Hz}$, $f_8 = 2518.9 \text{ Hz}$. The relationship between dimensionless and natural eigenvalues (λ_i and ω_i , respectively) of the fixed-fixed beam is given by the formula (cf. [9, p. 78])

$$\lambda_i = \kappa_i \ell = \sqrt{\omega_i} \left(\frac{\rho A}{EI} \right)^{1/4} \ell. \quad (56)$$

With this formula, we convert the natural eigenvalues ω_i to dimensionless eigenvalues λ_i : $\lambda_1 = 4.730041$, $\lambda_2 = 7.853205$, $\lambda_3 = 10.995608$, $\lambda_4 = 14.137165$, $\lambda_5 = 17.278760$, $\lambda_6 = 20.420352$, $\lambda_7 = 23.561944$, $\lambda_8 = 26.703522$. The calculated frequencies are in good agreement with the results obtained in [63, p. 7.15].

To apply a *nodal load*, we divide the beam into two elements (Fig. 7). The natural frequencies of the fixed-fixed beam with two elements are equal to the frequencies found with one element (Fig. 5).

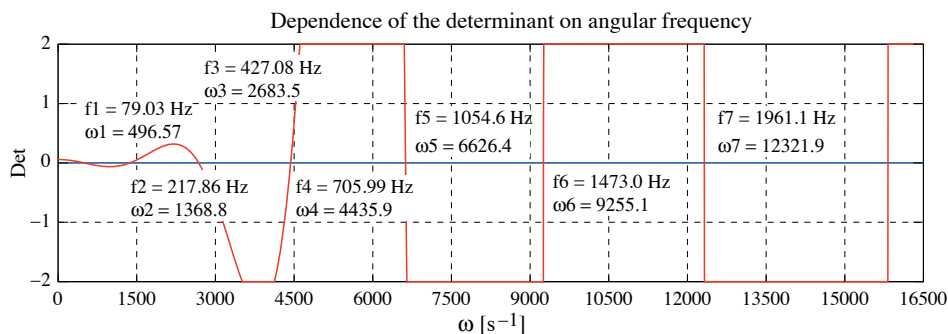


Fig. 6. Natural frequencies of fixed-fixed beam.

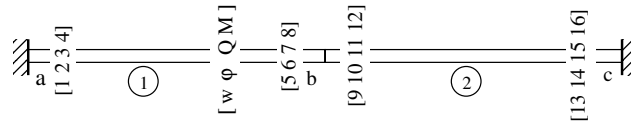


Fig. 7. Displacement and force indices of fixed-fixed beam elements.

The components of the state vector $Z(i)$ ($i = 1, 2, 3, \dots, 16$) (cf. $\Phi(i)$ in Eq. (2)) in index notation are shown in Fig. 7. In the system of EST-method equations (52), the first eight equations represent the basic equation (39) of the method. The following four equations represent compatibility of the displacements and joint equilibrium at node b :

$$\begin{aligned}
 w_L^{(ab)} - w_A^{(bc)} &\equiv Z(5) - Z(9) = 0, \\
 \varphi_L^{(ab)} - \varphi_A^{(bc)} &\equiv Z(6) - Z(10) = 0, \\
 Q_L^{(ab)} + Q_A^{(bc)} &\equiv Z(7) + Z(11) = F_b, \\
 M_L^{(ab)} + M_A^{(bc)} &\equiv Z(8) + Z(12) = 0.
 \end{aligned}
 \tag{57}$$

Now we apply the boundary conditions as restrictions on support displacements:

$$\begin{aligned}
 w_A^{(ab)} &\equiv Z(1) = 0, \\
 \varphi_A^{(ab)} &\equiv Z(2) = 0, \\
 w_L^{(bc)} &\equiv Z(13) = 0, \\
 \varphi_L^{(bc)} &\equiv Z(14) = 0.
 \end{aligned}
 \tag{58}$$

The sparsity pattern of the coefficient matrix spA of Eqs (52) of the fixed-fixed beam with two elements (Fig. 7) is shown in Fig. 8.

For the nontrivial solution of the homogeneous system (52), we will choose a free variable in accordance with the natural frequency ω_i (see program script excerpt 2.1).

The first mode shapes are found with a GNU Octave script. We divide the beam of length ℓ into two elements of lengths ℓ_1 and ℓ_2 (see program script excerpt 2.1). The fifth column is shifted to the right-hand side and the equations are solved with the least-squares method. After finding the initial parameters, we compile the mode shapes.

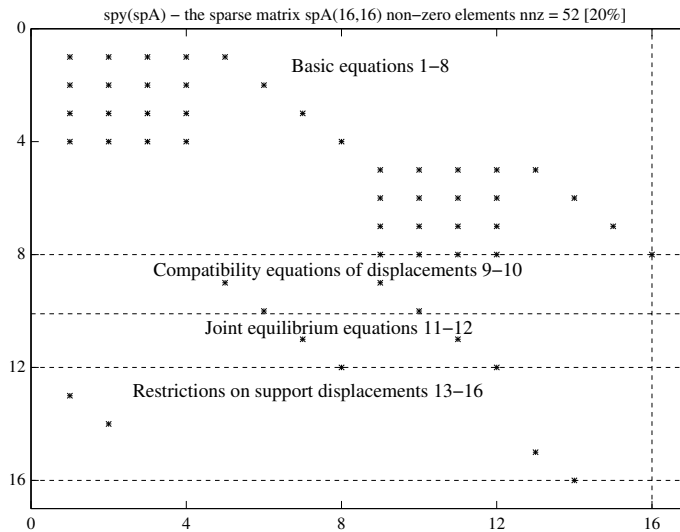


Fig. 8. Sparsity pattern of matrix spA of the fixed-fixed beam.

Program excerpt 2.1 (TalaKahelToelFFshape.m)

```

#CHOOSE A FREQUENCY wfs:
%wfs=496.574977  ## case{1} Mode shape 1      # wfHz = 79.032
wfs=1368.8280469  ## case{2} Mode shape 2    # wfHz = 217.86
%wfs=2683.450276  ## case{3} Mode shape 3    # wfHz = 427.08
%wfs=4435.8796194  ## case{4} Mode shape 4   # wfHz = 705.99
%wfs=6626.438860  ## case{5} Mode shape 5   # wfHz = 1054.6
%wfs=9255.1087056  ## case{6} Mode shape 6   # wfHz = 1473.0

if (wfs == 496.574977)
    ModeShape=1
    l1=0.11450; %% l=0.229 # m
    l2=0.11450;
    columns_to_remove = [5];
    ScaleMultiplier=1.0e-00
    titlJ=1;
elseif (wfs == 1368.8280469)
    ModeShape=2
    l1=0.06870;
    l2=0.16030;
    columns_to_remove = [5];
    ScaleMultiplier=0.99e-00
    titlJ=2;
elseif (wfs == 2683.450276)
    ModeShape=3
    l1=0.11450;
    l2=0.11450;
    columns_to_remove = [5];
    ScaleMultiplier=0.92e-00
    titlJ=3;
elseif (wfs == 4435.8796194)
    ModeShape=4
    l1=0.034350;
    l2=0.194650;
    columns_to_remove = [5];
    ScaleMultiplier=1.0e-00
    titlJ=4;
    disp(' ModeShape 4 ')
elseif (wfs == 6626.438860)
    ModeShape=5
    l1=0.034350;
    l2=0.194650;
    columns_to_remove = [5];
    ScaleMultiplier=0.95e-00
    titlJ=5;
elseif (wfs == 9255.1087056)
    ModeShape=6
    l1=0.06870;
    l2=0.16030;
    columns_to_remove = [5];
    ScaleMultiplier=-0.75e-00
    titlJ=6;
endif

```

Figure 9 depicts the four displacement mode shapes of the fixed-fixed beam.

Steady-state forced vibration can be represented by response curves [28] with the eigenvalues (saddle and star points) lying on the abscissa axis and the transversal displacement and elastic strain energy amplitudes on the ordinate axis [29, p. 143].

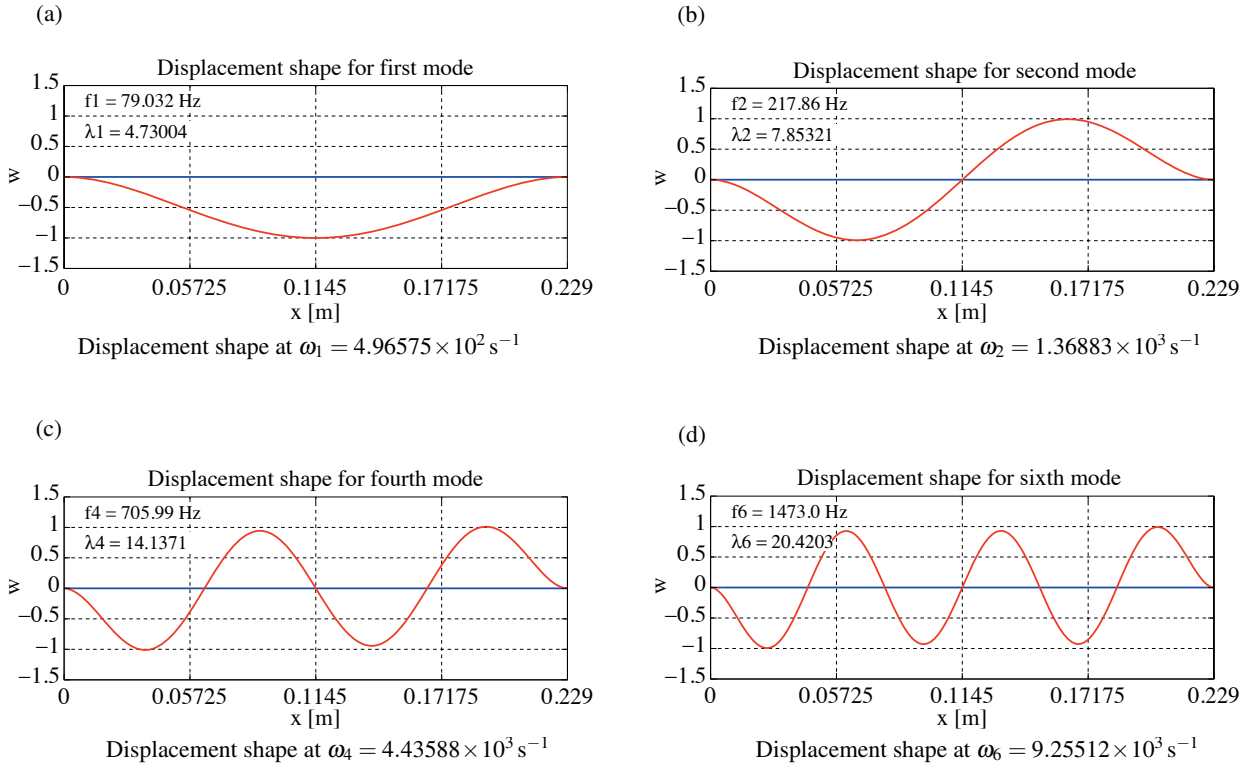


Fig. 9. Transversal displacement shapes of fixed-fixed beam modes.

In the real/actual work $W_i^{(a)}$ of internal forces, the kinematically admissible displacements are

$$W_i^{(a)} = -\mathcal{U} = -\int_0^\ell \frac{Q_z \hat{Q}_{zk}}{2GA_{red}} dx - \int_0^\ell \frac{M_y \hat{M}_{yk}}{2EI_y} dx, \quad (59)$$

where \mathcal{U} is the elastic strain energy; GA_{red} is the shear stiffness of a beam, and EI_y is the flexural rigidity of a beam.

The elastic energy \mathcal{U} of a fixed-fixed beam calculated with Simpson's rule:

$$\begin{aligned} \mathcal{U}_{sum} = & \frac{\Delta\ell}{3 \cdot 2GA_{red}} (f1(1)^2 + 4f1(2)^2 + 2f1(3)^2 + 4f1(4)^2 + 2f1(5)^2 + 4f1(6)^2 + 2f1(7)^2 \\ & + 4f1(8)^2 + f1(9)^2 + f1(10)^2 + 4f1(11)^2 + 2f1(12)^2 + 4f1(13)^2 + 2f1(14)^2 \\ & + 4f1(15)^2 + 2f1(16)^2 + 4f1(17)^2 + f1(18)^2) \\ & + \frac{\Delta\ell}{3 \cdot 2EI_y} (f2(1)^2 + 4f2(2)^2 + 2f2(3)^2 + 4f2(4)^2 + 2f2(5)^2 + 4f2(6)^2 + 2f2(7)^2 \\ & + 4f2(8)^2 + f2(9)^2 + f2(10)^2 + 4f2(11)^2 + 2f2(12)^2 + 4f2(13)^2 + 2f2(14)^2 \\ & + 4f2(15)^2 + 2f2(16)^2 + 4f2(17)^2 + f2(18)^2), \end{aligned} \quad (60)$$

where $\Delta\ell = \ell/16$ and $f1(n) = Q_z(0 + (n-1)\Delta\ell)$, $n = 1, 2, 3, \dots, 9$, $f1(m) = Q_z(0.5\ell + (m-10)\Delta\ell)$, $m = 10, 11, 12, \dots, 18$ ($f1(9) = Q_z(0.5\ell - \epsilon)$, $f1(10) = Q_z(0.5\ell + \epsilon)$); $f2(n) = M_y(0 + (n-1)\Delta\ell)$, $n = 1, 2, 3, \dots, 9$, $f2(m) = M_y(0.5\ell + (m-10)\Delta\ell)$, $m = 10, 11, 12, \dots, 18$ ($f2(9) = M_y(0.5\ell - \epsilon)$, $f2(10) = M_y(0.5\ell + \epsilon)$).

To construct response curves, we use the particular solution $\mathbf{Z}_p = \mathbf{Z}_F$ (Eq. (35)). After finding the initial parameters, the displacements and forces are found with the transfer equations (37).

The star points are related to resonance [54, p. 521], and that is why the amplitude increases steadily, approaching infinity.

Figures 10a,b show the steady-state frequency response curves of the fixed-fixed beam in the following intervals of frequency ω :

$$\underbrace{\varepsilon < \omega < \omega_1 - \varepsilon}_{1st\ interval}, \underbrace{\omega_1 + \varepsilon < \omega < \omega_2 - \varepsilon}_{2nd\ interval}, \underbrace{\omega_2 + \varepsilon < \omega < \omega_3 - \varepsilon}_{3rd\ interval}, \dots, \underbrace{\omega_n + \varepsilon < \omega < \omega_{n+1} - \varepsilon}_{nth\ interval}, \quad n = 1, 2, 3, \dots, 7.$$

On the frequency axis, the singular points 1, 3, 5, 7 are star points and 2, 4, 6 are saddle points.

On the frequency axis (ω -axis) (Fig. 10), the location of the natural frequencies ω_k matches that of the singular points lying on the same axis. Here the natural frequencies ω_k with $k = 1, 3, 5, \dots$ are double real auxiliary roots (Eq. (18)). Calculations show that near the singular points of odd numbers, the equilibrium state is changing rapidly and *signs of the amplitudes become reverse*. The singular points are *star points*; the equilibrium state is unstable. The elastic energy changes rapidly towards the maximum (see Fig. 10b).

Also located on the frequency axis (Fig. 10) are the natural frequencies ω_k ($k = 2, 4, 6, \dots$), which are double imaginary auxiliary roots (Eq. (18)). Calculations show that near the singular points of even numbers, the equilibrium state is changing slowly and *signs of the amplitudes become reverse*. The singular points are *saddle points*. The equilibrium state is marginally stable (*neutral/indifferent*) (see Fig. 10b).

The neighbourhood of double imaginary characteristic roots in saddle points needs further investigation. In saddle points, the pumping frequencies periodically shift “harmonics” [41, p. 18]. It is important to perceive if there exist regions of “undetermined” states of equilibrium with the so-called “parasitic self-excitation” (cf. gain of the pumping frequencies in saddle points). This phenomenon appears and disappears, often caused by tiny variations of the parameters in these regions of equilibrium states [64, p. 658].

The saddle points are associated with dynamic vibration absorption described in [65] for LTI systems.

In Figs 11 and 12, the deflection, slope, shear force and bending moment amplitudes at saddle point frequencies (the LTP system theory) of a fixed-fixed beam under steady-state forced vibrations are shown.

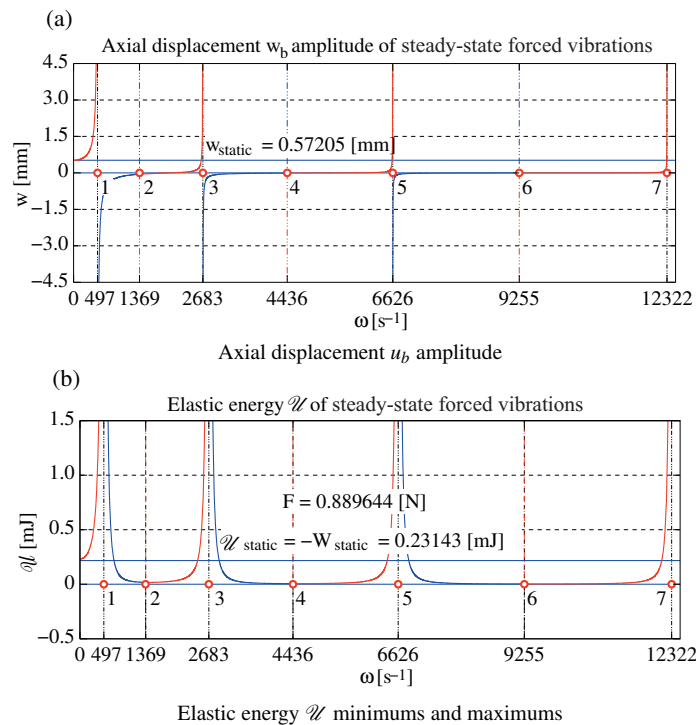


Fig. 10. Steady-state frequency response curves of fixed-fixed beam.

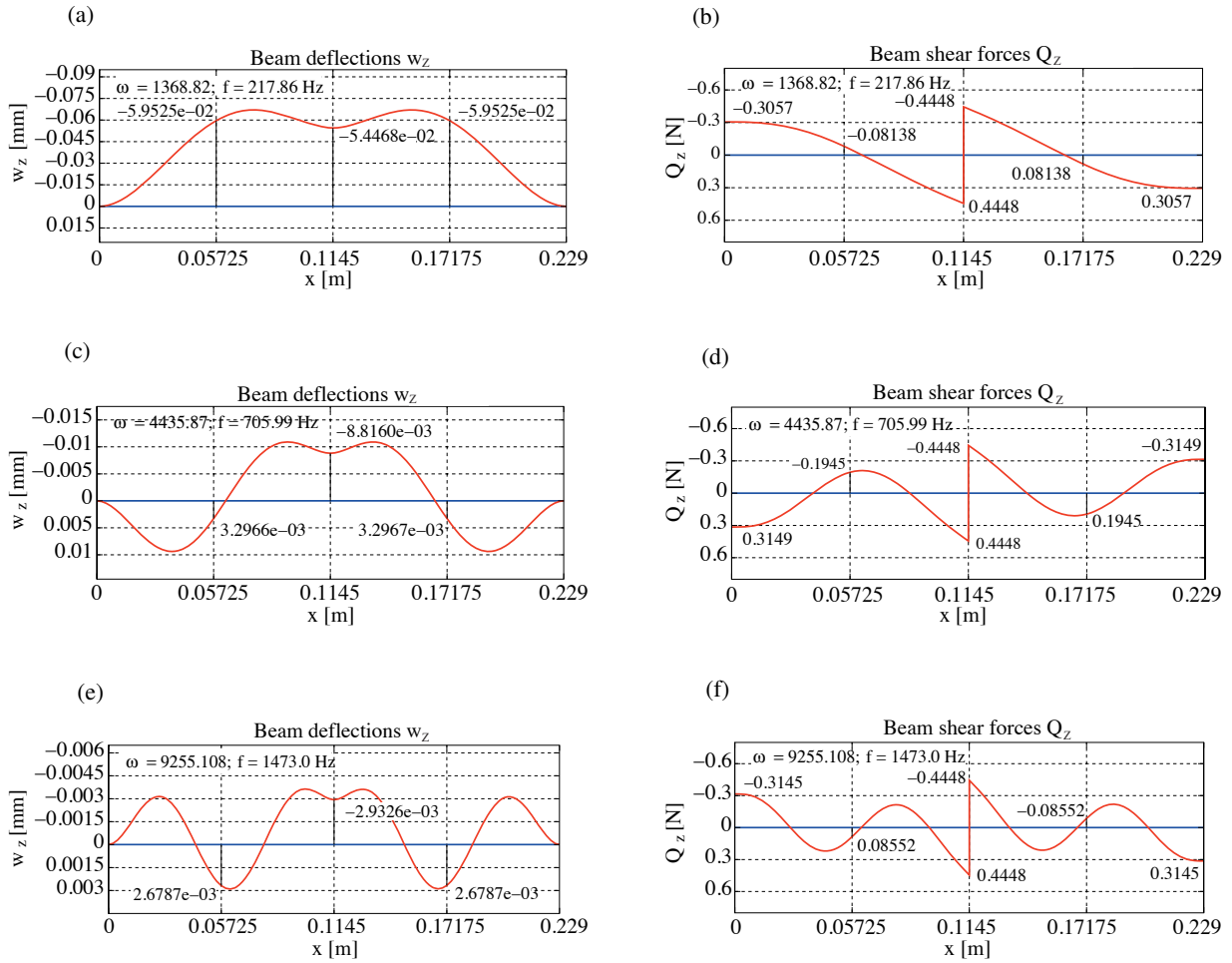


Fig. 11. Fixed-fixed beam deflection and shear force amplitudes at saddle point frequencies.

Here work done by constraint forces, e.g., support reactions, internal reactions (the contact force acts at the interconnection interface), is of zero value: $W_{boundaries} = [Q_z w_z + M_y \phi_y]_a^b = 0$.

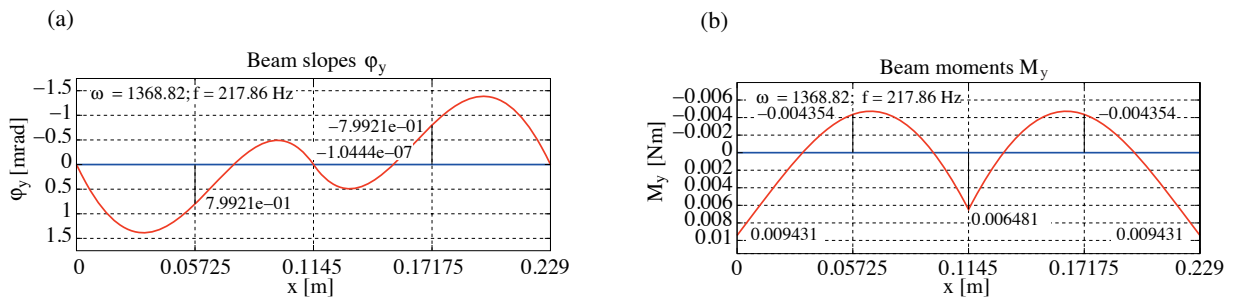


Fig. 12. Fixed-fixed beam slope and bending moment amplitudes at saddle point frequencies. (Continued on the next page.)

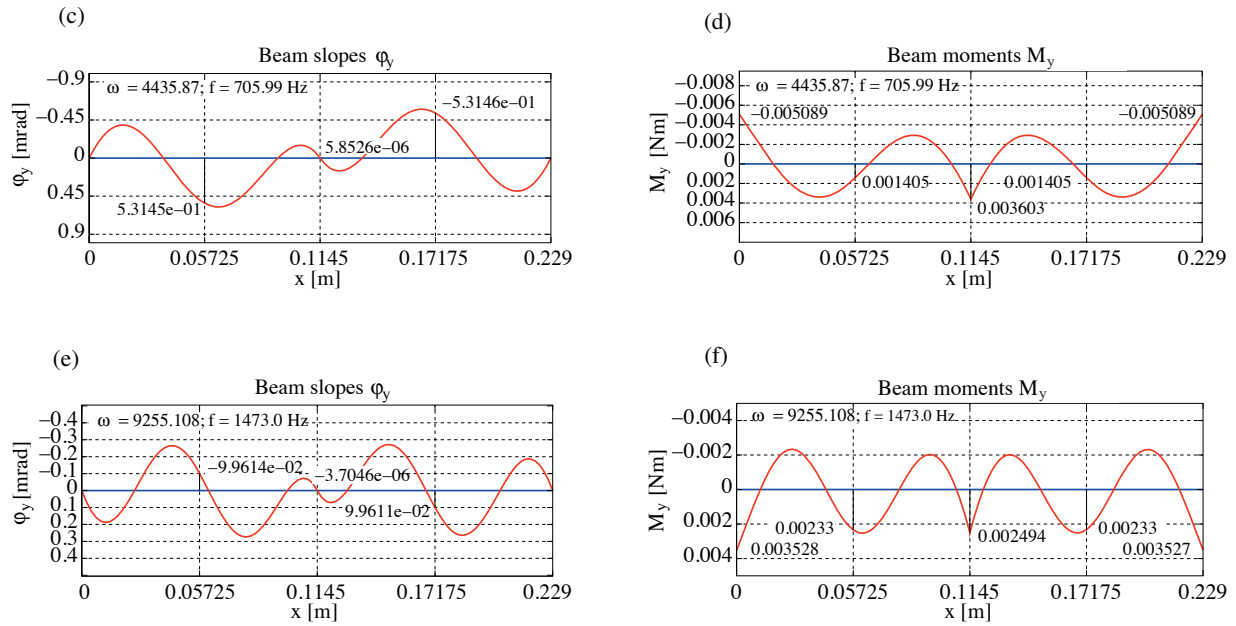


Fig. 12. Continued.

Figure 13 illustrates the amplitudes of displacements and forces of the fixed-fixed beam at 60 Hz frequency.

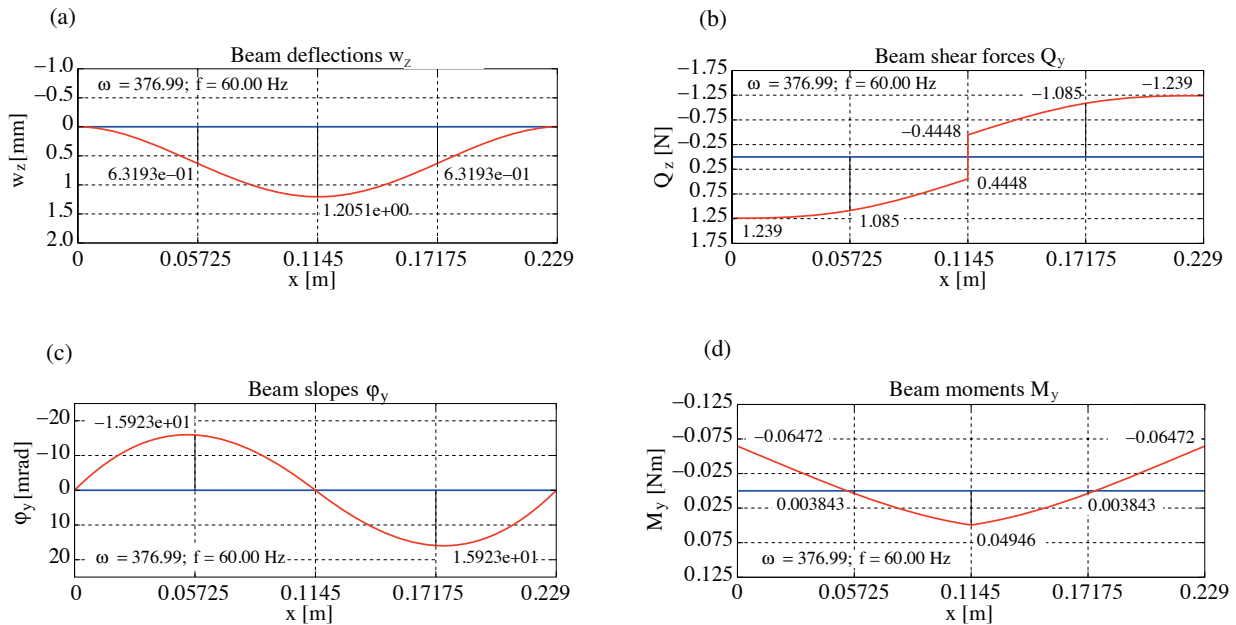


Fig. 13. Amplitudes of displacements and forces at 60 Hz frequency.

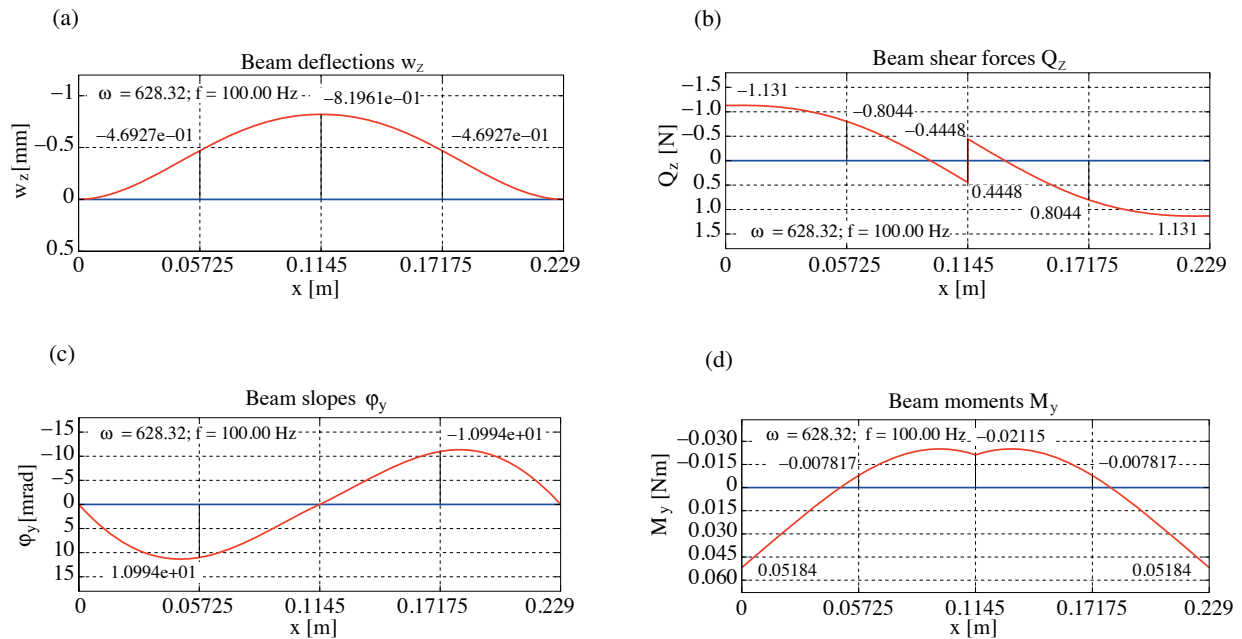


Fig. 14. Amplitudes of displacements and forces at 100 Hz frequency.

Figure 14 illustrates the amplitudes of displacements and forces of the fixed-fixed beam at 100 Hz frequency.

3. CONCLUSIONS

A modified transfer matrix method has been developed for solving the systems of first order differential equations for vibration with a set of initial values and boundary conditions. Steady-state frequency response curves of a beam are composed with singular points (star and saddle points) lying on the frequency axis of the response curves. At these points, the frequencies coincide with these determined by the homogeneous differential equation. Star points represent resonance frequencies. In the case of undamped vibration, dynamic vibration absorption takes place at saddle points.

ACKNOWLEDGEMENT

The publication costs of this article were covered by the Estonian Academy of Sciences.

REFERENCES

1. Lahe, A., Braunbrück, A., and Klauson, A. Modified transfer matrix method for steady-state forced vibration: a system of bar elements. *Proc. Estonian Acad. Sci.*, 2020, **69**(2), 143–161. <https://doi.org/10.3176/proc.2020.2.06>
2. Pestel, E. C. and Leckie, F. A. *Matrix Method in Elastomechanics*. McGraw-Hill, New York, 1963.
3. Den Hartog, J. P. *Mechanical Vibrations, 4th Edition*. Dover Publications, Inc., New York, 1985.
4. Pani, S., Senapati, K., Patra, K. C., and Nath, P. Review of an effective dynamic vibration absorber for a simply supported beam and parametric optimization to reduce vibration amplitude. *Int. J. Eng. Res. Appl.*, 2017, **7**(7), Part III, 49–77. <https://doi.org/10.9790/9622-0707034977>
5. He, B., Rui, X., and Zhang, H. Transfer matrix method for natural vibration analysis of tree system. *Math. Probl. Eng.*, **2012**, Article ID 393204. <https://doi.org/10.1155/2012/393204>

6. Lahe, A. The transfer matrix and the boundary element method. *Proc. Estonian Acad. Sci. Eng.*, 1997, **3**(1), 3–12. <http://books.google.ee/books?id=ghco7svk5T4C&pg=PA3&lpg=PA3&dq=Andres+Lahe&source=bl&ots=3SFfo4UCES&sig=%5FXLUez-SfW2FVYGRx8v2LVm16V8&hl=et&ei=YQaFTMeIEoWcOOyCyNwP&sa=X&oi=book%5Fresult&ct=result&resnum=5&ved=0CB0Q6AEwBDgK#v=onepage&q=Andres%20Lahe&f=false>
7. Lahe, A. *Ehitusmehaanika*. Tallinn University of Technology Press, Tallinn, 2012 (in Estonian). <https://digi.lib.ttu.ee/i/?793>
8. Lahe, A. *The EST Method: Structural Analysis*. Tallinn University of Technology Press, Tallinn, 2014. <https://digi.lib.ttu.ee/i/?1717>
9. Lahe, A. *Varrassüsteemide võnkumine. EST-meetod*. Tallinn University of Technology Press, Tallinn, 2018 (in Estonian). <https://digi.lib.ttu.ee/i/?9708>
10. Krätzig, W. B., Harte, R., Meskouris, K., and Wittek, U. *Tragwerke 1. Theorie und Berechnungsmethoden statisch bestimmter Stabtragwerke*. Springer-Verlag, Berlin, Heidelberg, 2010. <https://doi.org/10.1007/978-3-642-12284-2>
11. Argyris, J. H. and Mlejnek, H.-P. *Dynamics of Structures, Vol. 5*. Elsevier Science Publishers B.V., North-Holland, 1991.
12. Haberman, R. *Elementary Applied Partial Differential Equations*. Prentice-Hall International, New Jersey, 1983.
13. Yang, S. Modal identification of linear time periodic systems with applications to Continuous-Scan Laser Doppler Vibrometry. PhD thesis. University of Wisconsin-Madison, Wisconsin, 2013.
14. Kiselev, V. A. *Special Course. Dynamics and Stability of Structures*. Strojizdat, Moscow, 1964 (in Russian).
15. Babakov, I. M. *The theory of vibrations, 2nd Edition*. Nauka, Moscow, 1965 (in Russian).
16. Karnovsky, I. A. and Lebed, O. *Advanced Methods of Structural Analysis*. Springer, Boston, 2010.
17. Karnovsky, I. A. and Lebed, E. *Theory of Vibration Protection*. Springer International Publishing, Cham, 2016.
18. Kang, B. Exact transfer function analysis of distributed parameter systems by wave propagation techniques. In *Recent Advances in Vibrations Analysis* (Baddour, N., ed.). IntechOpen, Rijeka, 2011, 1–27. <https://doi.org/10.5772/22379>
19. Allen, M. S., Sracic, M. W., Chauhan, S., and Hansen, M. H. Output-only modal analysis of linear time periodic systems with application to wind turbine simulation data. In *Structural Dynamics and Renewable Energy* (Proulx, T., ed.). Springer, New York, 2011, 361–374. Conference Proceedings of the Society for Experimental Mechanics Series. Springer, New York, NY, 2011. <https://doi.org/10.1007/978-1-4419-9716-6%5F33>
20. Wereley, N. M. Analysis and control of linear periodically time varying systems. PhD thesis. Massachusetts Institute of Technology, Cambridge, 1991. <https://dspace.mit.edu/handle/1721.1/13761>
21. Hagedorn, P. and DasGupta, A. *Vibrations and Waves in Continuous Mechanical Systems*. John Wiley & Sons, Chichester, 2007. <https://doi.org/10.1002/9780470518434>
22. Farlow, S. J. *Partial Differential Equations for Scientists and Engineers*. John Wiley & Sons, New York, 1993.
23. Curtain, R. and Morris, K. Transfer functions of distributed parameter systems: A tutorial. *Automatica*, 2009, **45**(5), 1101–1116. <https://doi.org/10.1016/j.automatica.2009.01.008>
24. Song, J., Huang, Q.-A. System-Level modeling of packaging effects of MEMS devices. In *System-Level Modeling of MEMS* (Bechtold, T., Schrag, G., and Feng, L., eds). Wiley-VCH Verlag GmbH & Co. KGaA, 2013, 147–160. <https://doi.org/10.1002/9783527647132.ch6>
25. Pilkey, W. D. and Wunderlich, W. *Mechanics of Structures: Variational and Computational Methods*. CRC Press, Boca Raton, 1994.
26. Lahe, A., Braunbrück, A., and Klauson, A. An exact solution of truss vibration problems. *Proc. Estonian Acad. Sci.*, 2019, **68**(3), 244–263. <https://doi.org/10.3176/proc.2019.3.04>
27. Avcar, M. Free vibration analysis of beams considering different geometric characteristics and boundary conditions. *Int. J. Mech. Appl.*, 2014, **3**(3), 94–100. <https://doi.org/10.5923/j.mechanics.20140403.03>
28. Rosenberg, R. Steady-state forced vibrations. *Int. J. Non-Linear Mech.*, Elsevier, 1966, **1**(2), 95–108. [https://doi.org/10.1016/0020-7462\(66\)90023-0](https://doi.org/10.1016/0020-7462(66)90023-0)
29. Sracic, M. W. *A new experimental method for nonlinear system identification based on linear time periodic approximations*. PhD thesis. University of Wisconsin-Madison, Wisconsin, 2011.
30. Allen, M. S., Kuether, R. J., Deaner, B., and Sracic, M. W. A numerical continuation method to compute nonlinear normal modes using modal reduction. In *53rd AIAA/ASME/ASCE/AHS/ASC Structures, Structural Dynamics and Materials Conference, Honolulu, Hawaii, April 23–26, 2012*. AIAA, 2012, **11**, 9548–9567. <https://doi.org/10.2514/6.2012-1970>
31. Kozień, M. S. Analytical Solutions of Excited Vibrations of a Beam with Application of Distribution. *Acta Phys. Pol. A*, 2013, **123**(6), 1029–1033. <https://doi.org/10.12693/APhysPolA.123.1029>
32. Henderson, J. P. Vibration analysis of curved skin-stringer structures having tuned elastomeric dampers. PhD thesis. School of The Ohio State University, 1972. <https://apps.dtic.mil/docs/citations/AD0758220>
33. Abu-Hilal, M. Forced vibration of Euler-Bernoulli beams by means of dynamic Green functions. *J. Sound Vib.*, 2003, **267**(2), 191–207. [https://doi.org/10.1016/S0022-460X\(03\)00178-0](https://doi.org/10.1016/S0022-460X(03)00178-0)
34. Langtangen, H. P. and Linge, S. Vibration ODEs. In *Finite Difference Computing with PDEs. Texts in Computational Science and Engineering*. Springer, Cham, 2017, 1–92. <https://doi.org/10.1007/978-3-319-55456-3>

35. Kartofelev, D. Nonlinear sound generation mechanisms in musical acoustics. PhD thesis. Tallinn University of Technology, Tallinn, 2014. <https://digi.lib.ttu.ee/i/?1219>
36. Irofti, D., Boussaada, I., and Niculescu, S.-I. Geometric vs. algebraic approach: A study of double imaginary characteristic roots in time-delay systems. *IFAC-PapersOnLine*, 2017, **59**(1), 1310–1315. <https://doi.org/10.1016/j.ifacol.2017.08.123>
37. Irofti, D., Boussaada, I., and Niculescu, S.-I. Some insights into the migration of double imaginary roots under small deviation of two parameters. *Automatica*, 2018, **88**, 91–97. <https://doi.org/10.1016/j.automatica.2017.11.015>
38. Sandberg, H., Möllerstedt, E., and Bernhardsson, B. Frequency-domain analysis of linear time-periodic systems. *IEEE Trans. Autom. Control*, **50**(12), 1971–1983, 2005. <https://doi.org/10.1109/TAC.2005.860294>
39. Blin, N., Riedinger, P., Daafouz, J., Grimaud, L., and Feyel, P. A comparison of harmonic modeling methods with application to control of switched systems with active filtering. In *Proceedings of the 18th European Control Conference (ECC), Naples, Italy, June 25–28, 2019*. IEEE, 2019, 4198–4203. <https://doi.org/10.23919/ECC.2019.8796168>
40. Wereley, N. M. and Hall, S. R. Frequency response of linear time periodic systems. In *Proceedings of the 29th IEEE Conference on Decision and Control, Honolulu, HI, USA, December 5–7, 1990*. IEEE, 1991, 3650–3655. <http://doi.org/10.1109/CDC.1990.203516>
41. Siddiqi, A. Identification of the Harmonic Transfer Functions of a Helicopter Rotor. MSc thesis. Massachusetts Institute of Technology, Cambridge, 2001. <https://dspace.mit.edu/handle/1721.1/8900>
42. Tcherniak, D., Yang, S., and Allen, M. S. Experimental characterization of operating bladed rotor using harmonic power spectra and stochastic subspace identification. In *Proceedings of the 26th International Conference on Noise and Vibration Engineering (ISMA), Leuven, Belgium, September 15–17, 2014* (Sas, P., Moens, D., and Denayer, H., eds), 4421–4436.
43. Gbur, G. J. *Singular Optics*. CRC Press, Boca Raton, 2016.
44. Freund, I. and Shvartsman, N. Wave-field phase singularities: The sign principle. *Phys. Rev. A*, 1994, **50**(6), 5164–5172. <https://doi.org/10.1103/PhysRevA.50.5164>
45. Dias, C. A. N. General exact harmonic analysis of in-plane timoshenko beam structures. *Lat. Am. J. Solids Struct.*, 2014, **11**(12). <https://doi.org/10.1590/S1679-78252014001200004>
46. Yavari, A., Sarkani, S., and Moyer, E. T. Jr. On applications of generalized functions to beam bending problems. *Int. J. Solids Struct.*, 2000, **37**(40), 5675–5705. [https://doi.org/10.1016/S0020-7683\(99\)00271-1](https://doi.org/10.1016/S0020-7683(99)00271-1)
47. Dong, Y. and Liu, J. Exponential stabilization of uncertain nonlinear time-delay systems. *Adv. Difference Equations*, 2012, **180**. <https://doi.org/10.1186/1687-1847-2012-180>
48. Gu, K., Irofti, D., Boussaada, I., and Niculescu, S. Migration of double imaginary characteristic roots under small deviation of two delay parameters. In *Proceedings of the 54th IEEE Conference on Decision and Control (CDC), Osaka, Japan, December 15–18, 2015*. IEEE, 2016, 6410–6415. <https://doi.org/10.1109/CDC.2015.7403229>
49. Yin, H. and Tao, R. Improved transfer matrix method without numerical instability. *Europhys. Lett.*, 2008, **84**(5). <https://doi.org/10.1209%2F0295-5075%2F84%2F57006>
50. Kadisov, G. M. *Dynamics and Stability of Structures*. Litres, St. Petersburg, 2015. <https://books.google.ee/books?id=e5QoCwAAQBAJ>
51. Karnovsky, I. A. *Theory of Arched Structures: Strength, Stability, Vibration*. Springer-Verlag, New York, 2012. <http://doi.org/10.1007/978-1-4614-0469-9>
52. Jürgenson, A. *Tugevusõpetus*. Valgus, Tallinn, 1985 (in Estonian). <http://digi.lib.ttu.ee/i/?472>
53. Structural Dynamics of Linear Elastic Single-Degree-of-Freedom (SDOF) Systems. Instructional Material Complementing FEMA 451, Design Examples. http://www.ce.memphis.edu/7119/PDFs/FEAM_Notes/Topic03-StructuralDynamicsofSDOFSystemsNotes.pdf
54. Crowell, B. *Mechanics*. Light and Matter, Fullerton, California, 2019. <http://www.lightandmatter.com/mechanics/>
55. Wen-Xi, H., Xiao, X. Y., Yun-Ling, J., and Dong-Fang, Y. Automatic segmentation method for voltage sag detection and characterization. In *Proceedings of the 18th International Conference on Harmonics and Quality of Power (ICHQP), Ljubljana, Slovenia, May 13–16, 2018*. IEEE, 2018, 1–5. <https://doi.org/10.1109/ICHQP.2018.8378821>
56. Murray, R. M., Li, Z., and Sastry, S. S. *A Mathematical Introduction to Robotic Manipulation*. CRC Press, Boca Raton–London–New York–Washington, D.C., 1994. <https://www.cds.caltech.edu/~murray/books/MLS/pdf/mls94-complete.pdf>
57. Smirnov, A. F., Aleksandrov, A. V., Lashchenikov, B. Ya., and Shaposhnikov, N. N. *Structural Mechanics. Dynamics and Stability of Structures*. Strojizdat, Moscow, 1984 (in Russian).
58. Stepanov, V. V. *Course of Differential Equations, 8th Edition*. Fizmatgiz, Moscow, 1959 (in Russian).
59. Gajic, Z. *Linear Dynamic Systems and Signals*. Prentice Hall, Upper Saddle River, 2003.
60. Yang, B. *Stress, Strain, and Structural Dynamics: An Interactive Handbook of Formulas, Solutions and MATLAB Toolboxes*. Elsevier Academic Press, Oxford, 2005. <https://doi.org/10.1016/B978-0-12-787767-9.X5000-4>
61. Coşkun, S. B., Atay, M. T., and Öztürk, B. Transverse Vibration Analysis of Euler-Bernoulli Beams Using Analytical Approximate Techniques. In *Advances in Vibration Analysis Research* (Ebrahimi, F., ed.). IntechOpen, Rijeka, 2011, 1–22. <https://doi.org/10.5772/15891>

62. Walker, L. R. Finite element solution: nonlinear flapping beams for use with micro air vehicle design. MSc thesis. Air University. Air Force Institute of Technology, Ohio, 2007. <http://docplayer.net/129805126-Air-force-institute-of-technology.html>
63. Stokey, W. F. Vibration of systems having distributed mass and elasticity. In *Harris' Shock and Vibration Handbook, 5th Edition* (Harris, C. M. and Piersol, A. G., eds). McGraw-Hill, New York–Chicago–San Francisco, 2002.
64. Andronov, A. A., Vitt, A. A., and Khaikin, S. E. *Theory of Oscillator*. Pergamon Press, Oxford–London–Edinburg–New York–Toronto–Paris–Frankfurt, 1966. <https://doi.org/10.1002/zamm.19670470720>
65. Zilletti, M., Elliott, S. J., and Rustighi, E. Optimisation of dynamic vibration absorbers to minimise kinetic energy and maximise internal power dissipation. *J. Sound Vib.*, 2012, **331**(18), 4093–4100. <http://dx.doi.org/10.1016/j.jsv.2012.04.023>

Modifitseeritud ülekanemaatriksmeetod talasüsteemi sundvõnkumise uurimiseks

Andres Lahe

On välja töötatud EST-meetodi rakendus varrassüsteemide sundvõnkumise uurimiseks. Euleri-Bernoulli tala püsiseisundis võnkumise võrrandi üldlahendiga koostatakse võnkumise sagedustunnusjooned. Neil eristatakse kaht tüüpi singulaarpunkte: mittestabiilsed sõlmed (ingl *star points*) ja sadulpunktid (ingl *saddle points*). Varraste võnkumist kirjeldavad IV järku diferentsiaalvõrrandid asendatakse I järku diferentsiaalvõrrandite süsteemiga koos vastavate algväärtuste ja rajatingimustega. Diferentsiaalvõrrandite süsteemi lahendite uurimiseks on kasutatud modifitseeritud ülekanemaatriksmeetodit.